Journal of Applied Polymer Science

In Vitro Toxicity Evaluation of Hydrogel–Carbon Nanotubes Composites on Intestinal Cells

Romina Bellingeri,[1] Fabrisio Alustiza,[1] Natalia Picco,[1] Diego Acevedo,[2,3] Maria Alejandra Molina,[4] Rebeca Rivero,[2] Carolina Grosso,[1] Carlos Motta,[2] Cesar Barbero,[2] Adriana Vivas[1]

[1]Animal Biotechnology Laboratory, Department of Animal Anatomy, Faculty of Agronomy and Veterinary, National University of Rio Cuarto, Río Cuarto, Argentina

[2]Advanced Materials Laboratory, Department of Chemistry, Faculty of Exact, Physico-Chemical and Natural Sciences, National University of Río Cuarto, Río Cuarto, Argentina

[3]Department of Chemistry Technology, Faculty of Engineering, National University of Río Cuarto, Río Cuarto, Argentina

[4]Institute of Chemistry and Biochemistry, Freie Universität Berlin, Germany

Correspondence to: Dr. R. Bellingeri (E-mail: rbellingeri@ayv.unrc.edu.ar)

ABSTRACT: Composite materials based on carbon nanotubes (CNT) and polymeric hydrogels have become the subject matter of major interest for use as carriers in drug delivery research. The aim of this study was to evaluate the *in vitro* cytotoxicity of the hydrogel–carbon nanotube–chitosan (hydrogel–CNT–CH) composites on intestinal cells. Oxidized CNT were wrapped with chitosan (CH), Fourier transform infrared (FT-IR) analysis suggest that oxidized CNT interact with CH. Transmission electron microscopy (TEM) images show a CH layer lying around CNT. Chitosan wrapped CNT were incorporated to poly (acrylamide-co-acrylic acid) hydrogels. Swelling behavior in buffers at different pH were evaluated and revealed a significantly lower swelling when it is exposed to a acid buffer solution (pH 2.2). Mechanical properties were evaluated by measurements of elasticity and the material with CNT showed better mechanical properties. The incorporation and liberation of Egg Yolk Immunoglobulin from hydrogel–CNT–CH were also assessed and it revealed an improved performance. To evaluate the effect of these nanocomposites on cellular redox balance, intestinal cells were exposed to hydrogel–CNT–CH composites and antioxidant enzymes were assessed. Cytotoxicity and apoptosis were also evaluated. Hydrogel–CNT–CH composites induce no oxidative stress and there were no evidence of cytotoxicity or cell death. These preliminary findings suggest that hydrogel–CNT–CH composites show improved properties and good biocompatibility *in vitro* making these biomaterials promising systems for drug delivery purposes. © 2014 Wiley Periodicals, Inc. J. Appl. Polym. Sci. **2015**, *132*, 41370.

KEYWORDS: biocompatibility; composites; gels; graphene and fullerenes; nanotubes

Received 10 March 2014; accepted 1 August 2014
DOI: 10.1002/app.41370

INTRODUCTION

In recent years, hydrogels have emerged as promising biomaterials due to their unique characteristics. These polymeric networks, indeed, resemble living tissues closely in their physical properties because of their relatively elastomeric and soft nature and high water content, minimizing mechanical and frictional irritation.[1–3] Recently, it has reached tremendous importance in wide variety of biomedical applications including drug delivery, tissue engineering, and hyperthermia treatment.[4–7] However, these applications are often limited due to their poor mechanical and limited response properties, incomplete release of the therapeutic agent and the poor scalability of the manufacturing process represent other limitations.[8] In the aim to overcome these drawbacks, hydrogel nanocomposites have been developed enhancing mechanical strength, drug release profile, remote actuation capabilities, and biological interactions due the combination of the component properties in the hybrid network.[9–12] The employment of carbon nanotubes (CNT) as drug excipients with low toxicity and immunogenicity was reported in the aim to obtain innovative drug vehicles to be applied in the field of nanomedicine.[13,14] All the above-mentioned considerations clearly highlight the novelty of the use of composite materials based on CNT and polymeric hydrogels to be applied as innovative drug delivery devices.

Most of polymeric materials present a good biocompatibility and are suitable for biomedical applications.[15–17] However, the literature available on hydrogel nanocomposites biocompatibility is minimal. CNT may be considered the most important

constituent in the present hydrogel nanocomposites and they are also of the greatest concern on evaluating the toxicity of these system.[12,18]

In this study, an evaluation of the cytotoxicity of hydrogel–CNT–CH composites on intestinal cells is presented. Chitosan-wrapped CNT were incorporated to hydrogel to enhance the properties of these nanocomposites. A reduced swelling of nanocomposites in acid pH was revealed. The incorporation and liberation of IgY from these composites were also improved with the addition of CNT as well as the elastic modulus. *In vitro* cytotoxicity studies indicated that hydrogel–CNT–CH composites generate no alterations in cellular redox equilibrium, toxicity, or apoptosis. This approach contributed to the limited data available on the biocompatibility of hydrogel–CNT–CH composites.

MATERIAL AND METHODS

Carbon Nanotubes

Multiwalled CNT were obtained from Sun Nanotech, China. They were synthesized by chemical vapor deposition, with a purity >90% and residues <5% and 10–30 nm of diameter. Before use, 2.5 g of MWNTs were oxidized in 26 mL of 3 : 1 molar ratio acid solution (H_2SO_4 : HNO_3) for 3 h at 80°C with magnetic stirring. The MWNTs were then washed with deionized water until a pH of 7 was obtained, after which the samples were dried for 24 h at 100°C.

Decoration of Carbon Nanotubes with Chitosan

Chitosan (CH; ≥75% deacetylation, MW = 100 KDa) was provided by Sigma-Aldrich®.Surface decoration of CNT with CH was done dispersing 100 mg CNT in 100 mL CH solution (0.1 g CH dissolved in 100 mL 1% acetic acid solutions, pH = 2). The mixture was treated under an ultrasonic field for 10 min and then stirred for 1 h. During this step, CH macromolecules were adsorbed on the surface of the CNT thereby acting as polymer cationic surfactant to stabilize the CNT.[19] The wrapping were verified by examining its stability in acetic acid-added aqueous solution

Characterization of CH-Wrapped CNT

Fourier transform infrared (FT-IR) spectroscopy was conducted using a spectrophotometer (Nicolet Impact 400). The samples (CNT, CH, and CNT–CH) were mixed with KBr (1% w/w), and pellets were prepared under hydraulic press force of 15 tn. Pellets were vacuum-dried at 35°C for 12 h. The transmission measurements were done in a spectral range of 400–4,000 cm^{-1} with a resolution of 4 cm^{-1}. The microstructure of the wrapped CNT was examined by transmission electron microscopy (TEM) (Siemens, Elmiskop 101) and the measurements of CNTs were performed using AxioVision software (Carl Zeiss; Oberkochen, Germany).

Synthesis of Hydrogel–CNT–CH Composites

Acrylamide (AAm, Aldrich) and acrylic acid (AAc, Aldrich) were used as monomers. The cross-linker used was N,N'-methylene bisacrylamide (BAAm, Roth). The redox initiator system used was made of ammonium persulfate (APS, Roth) and N,N,N′,N′-tetramethyl ethylene diamine (TEMED, Merck). Monomers and cross-linker were dissolved in distilled water, and then the solution was bubbled with nitrogen for 15 min. After that, a solution containing APS (0.001 g/mL) and TEMED (10 μL/mL) was added and the reaction mix was sealed. The free radical polymerization of the hydrogels was carried out in tuberculin syringes at room temperature (22°C) for 3 h. The extreme of the syringe was cut and the gel was expulsed and sectioned into similar pieces (~5 mm). The resulting gels were washed several times with distilled water during one week to remove all the unreacted monomers. The pH of the water was measured to verify that unreacted monomers were eliminated. Then, gels were dried at room temperature until they reached constant weight. Three different types of hydrogels were prepared: hydrogel, hydrogel–$CNT_{1\%}$ and hydrogel–$CNT_{5\%}$, in the last two groups a percentage of water was replaced by a solution of CH-wrapped CNT (1.3 mg/mL). All samples were sterilized at 121°C for 20 min in a pressurized steam autoclave before biocompatibility assays.

Characterization of Hydrogel–CNT–CH Composites

Swelling Studies. For the pH dependent swelling studies, hydrogels were incubated in buffer solutions ranging from pH 2.2 to 10 at room temperature for 24 h. For pH 2.2 buffer solution 0.2*M* KCl/0.2*M* HCl buffer was used, NaOH/KH_2PO_4/Na_2HPO_4 buffer for pH 7.4 and 0.1*M* $NaHCO_3$/NaOH buffer for pH 10. The pH values were checked precisely by a pH-meter. After 24 h, the hydrogels were withdrawn from the buffer solution, measured, and weighed after removal of excessive surface water by lightly blotting with a filter paper. Particle size was measured using a manual caliper taking the average of five measurements. The swelling percentage was calculated by using the following formula:

$$\text{Swelling } \% = [(W_s - W_d)/W_s] \times 100$$

where W_s represents the weight of the swollen state of the sample and W_d is the weight of dry sample. The geometric mean of particle size in each pH was compared with a non-parametric Kruskal-Wallis test.

Mechanical Properties. Mechanical properties of hydrated macroscale hydrogel constructs were determined by unconfined compression testing using a dynamic mechanical analyzer. The uniaxial compression testing was performed with a crosshead speed of 1 mm/min on circular samples with 8-mm diameter and 1.0–1.4 mm thickness until point of failure. The 5–15% strain region was used to measure the compressive modulus of the samples.

Drug Carrier Performance. To evaluate the performance of hydrogel–CNT–CH composites as drug carrier, the incorporation, and liberation of Egg Yolk Immunoglobulin was evaluated. These assay were performed as our previously study.[20]

Porcine Intestinal Cell Culture

Porcine intestinal cells were obtained following a previous study.[21] Cells were cultured in Williams E Medium (Life Technologies) supplemented with 10% heat-inactivated fetal calf serum (Natocor), 1% l-glutamine and 1% non-essential amino acids (Sigma). Cells were seeded into a 24-well tissue-culture plate (Nunc®) at approximately 5×10^5 cells mL^{-1} and were grown overnight at 37°C in a humidified 5% CO_2 atmosphere.

Figure 1. Acetic acid-added aqueous solutions of the CH-wrapped CNTs (right) and the pure CNTs (left). [Color figure can be viewed in the online issue, which is available at wileyonlinelibrary.com.]

After 24 h of cell attachment, plates were washed with 500 μL/well phosphate buffered saline (PBS) and the cells were incubated with hydrogel–$CNT_{1\%}$ (~0.65 μg/well CNT) or hydrogel–$CNT_{5\%}$ (~3.25 μg/well CNT) or with hydrogel alone for 24 h. A control group with untreated cells was included. After incubation, hydrogel composites were retired and cytotoxicity was assessed as outlined below.

Enzymatic Assays

Total superoxide dismutase (SOD) activity was determined by the method of Misra and Fridovich.[22] The catalase (CAT) activity assay, consisting of the spectrophotometric measurement of H_2O_2 breakdown measured at 240 nm, was performed following the method of Chance.[23] Glutathione peroxidase (GSH-Px) activity was assayed following the rate of NADPH oxidation at 340 nm by the coupled reaction with glutathione reductase (GSH-Rd).[24] The specific activity was determined using the extinction coefficient of NADPH (6.22 mM^{-1} cm^{-1}). GSH-Rd activity was determined spectrophotometrically measuring NADPH oxidation at 340 nm.[25] Protein concentration in the samples was estimated by the method of Bradford using bovine serum albumin as standard.[26]

Viability Assay

The mitochondrial functionality of the intestinal cells was evaluated by using the 3-[4,5-dimethylthiazol-2-yl]-2,3-diphenyl tetrazolium bromide (MTT) assay.[27]

Apoptosis Assessment

After treatment with the nanocomposites in serum-free medium for 24 h, cells seeded on coverslips were fixed in 4% paraformaldehyde in PBS for 30 min. The *in situ* TUNEL assay was then performed in accordance with the manufacturer's protocol for cultured cells (Millipore). Cells were counterstained with hematoxylin. Apoptosis of intestinal cells was quantified by the number of apoptotic nuclei in the total nuclei in 50 continuous microscopic fields under 400× magnification by using the following formula:

$$\text{Apoptosis \%} = (\text{apoptotic nuclei/total nuclei}) \times 100$$

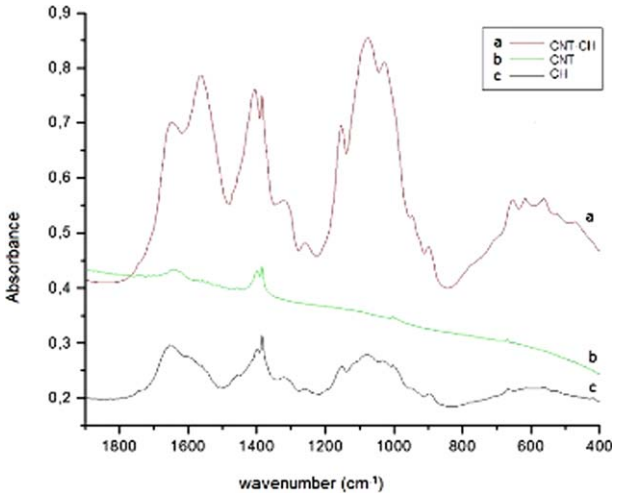

Figure 2. FTIR spectrum of: (a) CH-wrapped carbon nanotube (CNT–CH), (b) pure carbon nanotube (CNT), and (c) pure CH. [Color figure can be viewed in the online issue, which is available at wileyonlinelibrary.com.]

Statistical Analyses

Statistical analyses were performed using Infostat software.[28] Data were represented as means ± standard deviation (SD). Differences were considered significant at the level of $P < 0.05$. Levels of significance were evaluated by Kruskal-Wallis test.

RESULTS

Characterization of CH-Wrapped CNT

As can be seen in Figure 1, the CH-wrapped CNT form a stable dispersion in the acetic acid aqueous solution without precipitation, this dispersion is stable for up to 6 months while the CNT without CH aggregates and precipitates at the bottom in 1 h.

From the FT-IR spectrum [Figure 2(c)], it can be found the characteristics bands of CH absorption: at 1662 cm^{-1} (amide I), 1605 cm^{-1} (—NH_2 bending), and 1393 cm^{-1} (amide III). The absorption bands at 1164 cm^{-1} (asymmetric stretching of the CO—O—OC bridge), 1092, and 1042 cm^{-1} (skeletal vibration involving the COO stretching).[29] FT-IR of the oxidized CNTs [Figure 2(b)] show a band at 1550 cm^{-1}, most probably due to aromatic and unsaturated structural of C=C bonds, a band near 1410 cm^{-1} due to sorbed water (OH in-plane deformation) and overlapping bands in region characteristic for C—O moiety (e.g., C—O—C groups—oxides of structural, oxygen bridges, etc.). The C=O bands characteristic of carboxyl functional groups (—COOH) and of ketone/quinone are observed as a shoulder at 1711 and 1638 cm^{-1}, respectively.[30] On the other hand, FTIR spectrum of wrapped nanotubes [CNT–CH, Figure 2(a)] shows the bands that correspond not only to the CH but also the oxidized CNTs.

The microstructure of CNT–CH was observed by TEM. TEM measurements show that pristine CNTs present a thickness of

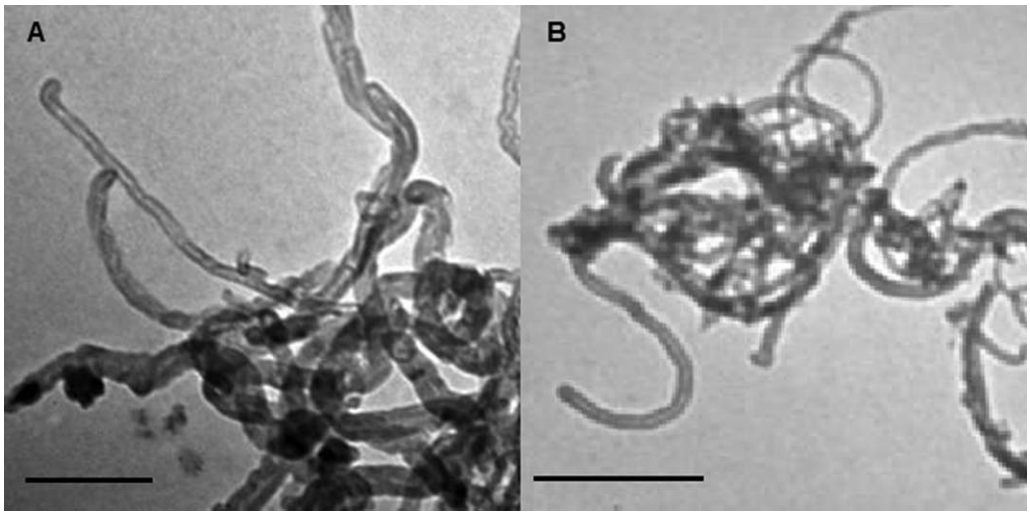

Figure 3. TEM images of: (a) pure carbon nantube (CNT) (scale bars = 200 nm, 1,20,000× Frame), (b) CH-wrapped carbon nanotube (CNT–CH) (scale bars = 500 nm, 40,000× Frame)

22.17 ± 3.38 nm, while the thickness of CNTs coated with CH is found to be 50.76 ± 1.43 nm (Figure 3).

Characterization of Hydrogel–CNT–CH Composites

Swelling Studies. Table I shows the values of size and swelling percentages of nanocomposites incubated for 24 h in buffers with different pH. Hydrogel–$CNT_{5\%}$ reveals a significantly smaller diameter and length when were exposed to a buffer solution of pH 2.2 ($P < 0.05$). In the same manner, the swelling percentage of hydrogel–$CNT_{5\%}$ composites has the less swelling percentage when it was incubated at pH 2.2 ($P < 0.05$). At pH 7.4 and 10, no differences between swelling performance of nanocomposites were founded (Table I).

Mechanical Properties. An unconfined compression test was performed to evaluate the mechanical properties of hydrogel–CNT–CH composites. The results indicated a significant increase in the compressive modulus of hydrogel–$CNT–CH_{5\%}$ (17.83 ± 0.50 KPa) and hydrogel–$CNT_{1\%}$ (16.85 ± 0.50 KPa) and compared with hydrogel alone (14.76 ± 0.50 KPa), ($P < 0.05$).

Drug Carrier Performance. The loading and liberation percentages of IgY from hydrogel–CNT–CH composites were assessed. Hydrogel–$CNT_{5\%}$ has the highest IgY loading percent ($P < 0.05$). It means that each composite tablet incorporated approximately 11.1 ± 2.3 mg IgY. Hydrogel–$CNT_{5\%}$ also shows a higher liberation percent of IgY liberating approximately 1.2 ± 2.3 mg IgY/tablet (Table II).

Oxidative Stress

The effect of nanocomposites on the most common and significant antioxidant enzymes was evaluated. CAT, SOD, GPx, and GRd were determined on intestinal cells after incubation with hydrogel–CNT–CH composites for 24 h. No significant differences across the groups could be detected (Table III).

Viability Assay

The effect of hydrogel–CNT–CH composites on MTT reduction was assessed. Figure 4 shows the relative amounts of viable cells in each group after the addition of hydrogel–CNT–CH composites. After 24 h in culture, no differences in cell viability across all the treatments compared with the control group.

Table I. Length, Diameter, and Swelling Percentage of Hydrogel–CNT–CH Composites Incubated in Buffers with Different pH

	Sample	pH 2.2	pH 7.4	pH 10
Length (mm)	Hydrogel	6.0 ± 0.1	6.2 ± 1.3	6.0 ± 0.1
	Hydrogel-$CNT_{1\%}$	4.0 ± 0.5	5.7 ± 1.5	6.3 ± 1.1
	Hydrogel-$CNT_{5\%}$	3.2 ± 0.3[a]	4.3 ± 0.6	6.3 ± 0.8
Diameter (mm)	Hydrogel	6.3 ± 1.0	10.0 ± 0.1	11.5 ± 0.2
	Hydrogel-$CNT_{1\%}$	5.0 ± 0.3	10.7 ± 0.6	11.5 ± 0.9
	Hydrogel-$CNT_{5\%}$	3.5 ± 0.1[a]	9.3 ± 0.6	12.0 ± 0.1
Swelling percentage (%)	Hydrogel	83.0 ± 2.7	97.0± 0.1	98.7 ± 0.6
	Hydrogel-$CNT_{1\%}$	59.0 ± 3.3	97.7 ± 0.6	98.3 ± 0.6
	Hydrogel-$CNT_{5\%}$	39.0 ± 2.0[a]	98.0 ± 0.1	99.0 ± 0.1

Data are represented as mean ± standard deviation (SD).
[a] Indicate significant difference ($P < 0.05$).
Kruskal–Wallis Test, Infostat, 2008.

Table II. Incorporation and Liberation of IgY from Hydrogel–CNT–CH Composites

	Incorporation percent (%)	Liberation percent (%)
Hydrogel	88.90 ± 8,92[a]	9.91 ± 1.06[a]
Hydrogel-$CNT_{1\%}$	102.05 ± 10.50[ab]	10.41 ± 0.84[a]
Hydrogel-$CNT_{5\%}$	131.33 ± 8.90[c]	15.16 ± 0.54[b]

Data are represented as mean ± standard deviation (SD).
Different letters indicate significant difference ($P < 0.05$).
Kruskal–Wallis Test, Infostat, 2008.

Apoptosis Assessment

Apoptosis was evaluated by TUNEL reaction analysis that measures DNA fragmentation. There are no significant differences between TUNEL-positive cell percents in different groups (Table IV).

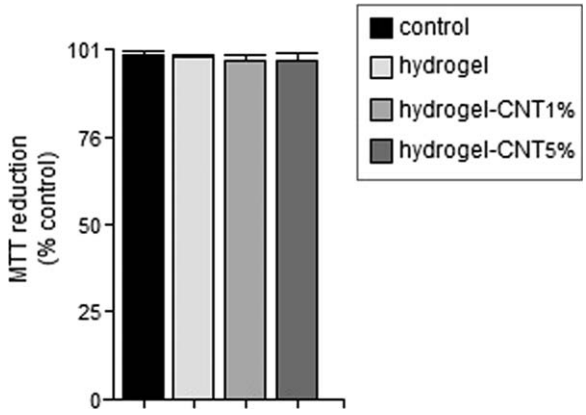

Figure 4. Cytotoxicity of hydrogel and nanocomposites to intestinal cells after 24 h exposure determined by the MTT assay. Data are expressed as percent of control mean ± SD of three independent experiments.

DISCUSSION

There is a limited data available on the compatibility of hydrogel nanocomposites. In this work, the effects of hydrogel–CNT–CH composites on intestinal cells were evaluated. The intestinal tract is particularly important in toxicology both as a target organ and as a site of access of xenobiotics into the organism.[31] In this work we employed a primary culture of porcine intestinal epithelial cells to evaluate the toxicity of these novels nanocomposites.

It is shown that defects can be created on the sidewalls as well as at the open ends of CNT by an oxidative process with strong acids such as HNO_3, H_2SO_4 or a mixture of them,[32] this groups generated on the CTNs allow a better interaction between this nanocompound and CH, as it can be seen in the FTIR spectrum. Wrapping of CNT with CH allows their desegregation and promote their uniform distribution in the medium and inside of the hydrogel, an important parameter which affect the mechanical properties of the final composite.[16,33] In this work, we used a method of non-covalent surface decoration of CNTs with CH. The FTIR and TEM imagines ensure that the wrapped of the CNTs with CH is an effective method to produce stable dispersion of CNTs.

In recent years, composite materials based on CNTs and polymeric hydrogels have become the subject matter of major interest for use as carriers in drug delivery research.[34,35] In this work, hydrogel–CNT–CH composites were synthesized to enhance the properties of the hydrogel alone. The results demonstrated that the properties of the hydrogel were improved significantly by adding CNTs. Particularly, an approximately 50% reduction of the swelling percentage of nanocomposites incubated on acid pH was achieved by the addition of only 5% v/v of CNTs. These nanocomposites also revealed an improved loading and liberation of IgY. Probably, a good dispersion of CNTs and the better interaction between CH and IgY in the matrix could lead to an efficient load transfer concentration centers in the nanocomposite.[36]

The literature on the mechanical properties of polymer nanotube composites explains the enhancement of mechanical properties by CNTs addition.[37] In this work, an increase in the elastic modulus of hydrogel–CNT–CH composites compared with hydrogel alone is observed probable due to the reinforcing effect of the CNTs within the hydrogels.[38] Due to the extraordinary mechanical properties of CNTs, small amounts of CNTs are sufficient to change considerably the mechanical properties of hybrid hydrogel–CNT–CH. It was seen that CNTs could dramatically decrease the size of pore. Normally, the smaller pore sizes indicated denser networks, which showed relatively higher mechanical strength.[39] Previous studies reveled an improvement of mechanical properties of poly(vinyl pyrrolidone) wrapped multiwalled carbon nanotube/poly(vinyl alcohol) composite hydrogels that became more wear-resistant in the presence of poly(vinyl pyrrolidone) with different CNT contents.[40] Previous studies have investigated the addition of CNT into CH hydrogels for the purpose of mechanical enhancement, and pH and electrical actuation. [41]

Table III. Enzymatic Values in Intestinal Cells After Incubation with Hydrogels and Nanocomposites for 24 h

Sample	CAT (K/mg protein)	SOD (USOD/mg protein)	GPx (K/mg protein)	GRd (K/mg protein)
Hydrogel	0.76 ± 0.19	20.11 ± 4.04	0.07 ± 0.03	0.24 ± 0.10
Hydrogel-$CNT_{1\%}$	0.73 ± 0.10	11.19 ± 1.28	0.11 ± 0.01	0.10 ± 0.05
Hydrogel-$CNT_{5\%}$	0.59 ± 0.11	23.68 ± 2.09	0.12 ± 0.03	0.19 ± 0.08
Control	0.93 ± 0.04	10.67 ± 2.60	0.10 ± 0.04	0.11 ± 0.05

Data are represented as mean ± standard deviation (SD).
Different letters indicate significant difference ($P < 0.05$).
Kruskal–Wallis Test, Infostat, 2008.

Table IV. TUNEL Positive Cell Percents After Incubation with Hydrogel–CNT–CH Composites

Treatment	TUNEL positive cells (%)
Control	3.67 ± 0.58^a
Hydrogel	4.00 ± 2.00^a
Hydrogel-$CNT_{1\%}$	5.33 ± 2.08^a
Hydrogel-$CNT_{5\%}$	5.67 ± 2.31^a

Data are represented as mean ± standard deviation (SD).
Different letters indicate significant difference ($P < 0.05$).
Kruskal–Wallis Test, Infostat, 2008.

Hydrogel nanocomposites have been demonstrated in numerous biomedical applications and remote controlled drug delivery systems.[42,43] However, to the best of our knowledge, few work has been reported so far on the biocompatibility of hydrogel–CNT–CH composites. The ability of nanomaterials to interact with biological tissues and generate reactive oxygen species (ROS) has been proposed as possible mechanisms involved in the toxicity.[44] In this study, we find that there is not a significant decrease in the activity of SOD, GSH-Px, and CAT. Biopersistence of CNTs and the potential to translocate through cells is a factor involved in sustained ROS generation and DNA damage.[45] However, in this study, CNT are shielded in some way by the polymer matrix. Moreover, the CH that covers CNT could be passivate their surface preventing further reactions. The functionalized CNT were reported to be able to penetrate mammalian cells without damaging the plasma membrane, and their accumulation did not show significant toxic effect on the cell cycle.[46] The generation of ROS caused by exposure to raw CNT containing redox active iron has been reported in human keratinocyte (HaCaT) cells.[47] Previous studies with iron-rich CNT caused a significant loss of glutathione and increased lipid peroxidation in murine alveolar macrophages.[48]

Cell viability studies using the MTT assay indicated hydrogel–CNT–CH composites do not cause a decline in cell viability. It is necessary note that the CNT concentration on hydrogel composites are lesser than those used in toxicology studies.[49] Similar results were obtained by Mejias Carpio et al. who evaluated the toxicity graphene-based nanocomposites and found that these materials presents excellent antibacterial properties without significant cytotoxicity to mammalian cells.[50] Previous studies about encapsulation of uncoated iron oxide nanoparticles within a poly(N-isopropylacrylamide) hydrogel showed that encapsulated iron exhibit a more favorable cell viability than the nanoparticles themselves suggesting that hydrogels can increase biocompatibility providing a barrier between sensitive tissues and the more harmful nanoparticles.[51]

CONCLUSION

The above mentioned results revealed that hydrogel–CNT–CH composites have an advantage related to the percentage of swelling on acid pH. The improved performance of the hydrogel–CNT–CH composite can be mainly attributed to the enhanced interactions between the polymer chains and nanoparticles. *In vitro* toxicity studies indicated that hydrogel–CNT–CH composites showed no signs of cytotoxicity on primary culture of porcine enterocytes probably, hydrogel matrix provide a shielding effect to CNTs. This work contributed to the limited data available on the biocompatibility of hydrogel nanocomposites.

AUTHOR CONTRIBUTIONS

R.B. designed the experiments, triggered viability and apoptosis assessment, and wrote the manuscript. F.A. and N.P. carried out swelling studies and evaluated the drug carrier performance of the nanocomposites. D.A. and M.A.M. collaborated to prepare the hydrogel–carbon nanotubes composites and carried out FT-IR analysis. C.G. and C.M. collaborated with the intestinal cells culture and enzymatic assays. R.R. carried out the analysis of mechanical properties of nanocomposites. C.B. advised about the decoration of CNTs and synthesis of hydrogel–carbon nanotubes composites. A.V. supervised the research. All the authors interpreted the data, critically revised the manuscript. and approved the final version.

ACKNOWLEDGMENTS

The authors thank CONICET. This work was supported by grants from Ministerio de Ciencia y Tecnología de Córdoba (MinCyT), Agencia Nacional de Promoción Científica y Tecnológica (FONCYT) and Secretaría de Ciencia y Técnica de la Universidad Nacional de Río Cuarto (SECYT-UNRC).

REFERENCES

1. Fisher, O. Z.; Khademhosseini, A.; Langer, R.; Peppas, N. A. *Acc. Chem. Res.* **2010**, *43*, 419.
2. Kloxin, A. M.; Kloxin, C. J.; Bowman, C. N.; Anseth, K. S. *Adv. Mater.* **2010**, *22*, 3484.
3. Cirillo, G.; Hampel, S.; Spizzirri, U. G.; Parisi, O. I.; Picci, N.; Iemma, F. *Biomed. Res. Int.* **2014**, DOI 10.1155/2014/825017.
4. Gibas, I.; Janik, L. *Chem. Chem. Technol.* **2010**, *4*, 297.
5. Li, Y.; Rodrigues, J.; Tomás, H. *Chem. Soc. Rev.* **2012**, *41*, 2193.
6. Seliktar, D. *Science* **2012**, *336*, 1124.
7. Schmidt, J. J.; Rowley, J.; Kong, J. *J. Biomed. Mater. Res.* **2008**, *87A*, 1113.
8. Crommelin, D.; Park, K.; Florence, A. *J. Control. Release* **2010**, *141*, 263.
9. Goenka, S.; Sant, V.; Sant, S. *J. Control. Release* **2014**, *173*, 75.
10. Yeum, J. H.; Park, S. M.; Kwon, J.; Kim, J. W.; Kim, Y. H. Rabbani, M. M.; Hyun, J. M.; Kim, K.; Oh, W. In Nanocomposites—New trends and developments; Ebrahimi, F., Ed.; InTech, **2012**; Chapter 2, DOI 10.5772/50485.
11. Satarkar, N. S.; Johnson, D.; Marrs, B.; Andrews, R.; Poh, C.; Gharaibeh, B.; Saito, K.; Anderson, K. W.; Hilt, J. Z. *J. Appl. Polym. Sci.* **2010**, *117*, 1813.
12. Meenach, S. A.; Anderson, K. W.; Hilt, J. Z. In Safety of Nanoparticles; Springer: New York, **2009**, p 131.
13. Foldvari, M.; Bagonluri, M. *Nanomedicine* **2008**, *4*, 183.

14. Zhang, Y.; Bai, Y.; Yan, B. *Drug Discov. Today* **2010**, *15*, 428.
15. Wu, J.; Wei, W.; Wang, L.; Su, Z.; Ma, G. *Biomaterials* **2007**, *28*, 2220.
16. Samchenko, Y.; Ulberg, Z.; Korotych, O. *Adv. Colloid. Interface Sci.* **2011**, *168*, 247.
17. Gaharwar, A. K.; Peppas, N. A.; Khademhosseini, A. *Biotechnol. Bioeng.* **2013**, *111*, 441.
18. Manke, A.; Wang, L.; Rojanasakul, Y. *BioMed. Res. Int.* **2013**, DOI 10.1155/2013/942916.
19. Liu, Y.; Tang, J.; Chen, X.; Xin, J. *Carbon* **2005**, *43*, 3178.
20. Fan, M. Z.; Stoll, B.; Jiang, R.; Burrin, D. G. *J. Anim. Sci.* **2001**, *79*, 371.
21. Bellingeri, R. V.; Picco, N. Y.; Alustiza, F. E.; Canova, V.; Molina, M. A.; Acevedo, D. F.; Barbero, C.; Vivas, A. B. *J. Food Sci. Technol.* **2014**, DOI 10.1007/s13197-014-1337-3.
22. Misra, H.; Fridovich, I. *J. Biol. Chem.* **1972**, *247*, 6960.
23. Chance, B. In Methods of Biochemical Analysis; Glick, D., Ed.; Interscience: New York, **1954**, p 408.
24. Flohé, L.; Gunzler, W. *Meth. Enzymol.* **1984**, *105*, 114.
25. Carlberg, I.; Mannervik, B. *Meth. Enzymol.* **1985**, *113*, 484.
26. Bradford, M. *Anal. Biochem.* **1976**, *72*, 248.
27. Mosmann, T. *J. Immunol. Methods* **1983**, *65*, 55.
28. Di Rienzo, J. A.; Casanoves, F.; Balzarini, M. G.; Gonzalez, L.; Tablada, M.; Robledo, C. W. **2008**, InfoStat, versión 2008, Grupo InfoStat, FCA, Universidad Nacional de Córdoba, Argentina.
29. Peniche, C.; ArguKelles-Monal, W.; Davidenko, N.; Sastre, R.; Gallardo, A.; San Roman, J. *Biomaterials* **1999**, *20*, 1869.
30. Stobinski, L.; Lesiak, B.; Kövér, L.; Tóth, J.; Biniak, S.; Trykowski, G.; Judek, J. *J. Alloy. Compd.* **2010**, *501*, 77.
31. Sambruy, Y.; Ferruzza, S.; Ranaldi, G.; DeAngelis, I. *Cell Biol. Toxicol.* **2001**, *17*, 301.
32. Esumi, K.; Ishigami, M.; Nakajima, A.; Sawada, K.; Honda, H. *Carbon* **1996**, *34*, 279.
33. Ma, P. C.; Siddiqui, N. A.; Marom, G.; Kim, J. K. *Compos. Appl. Sci. Manuf.* **2010**, *41*, 1345.
34. Cha, C.; Shin, S. R.; Annabi, N.; Dokmeci, M. R.; Khademhosseini, A. *ACS Nano* **2013**, *7*, 2891.
35. Vashist, A.; Vashist, A.; Gupta, Y. K.; Ahmad, S. *J. Mater. Chem. B* **2014**, *2*, 147.
36. Wang, Q.; Varadan, V. K. *Smart Mater. Struct.* **2005**, *14*, 281.
37. Coleman, J. N.; Khan, U.; Blau W. J.; Gun'ko Y. K. *Carbon* **2006**, *44*, 1624.
38. Wang, W.; Liao, S.; Liu, M; Zhao, Q.; Zhu, Y. *Int. J. Polym. Sci.* **2014**, 1.
39. Dai, T.; Qing, X.; Zhou, H.; Shen, C.; Wang, J.; Lu, Y. *Synth. Metals.* **2010**, *160*, 791.
40. Huang, Y.; Zheng, Y.; Song, W.; Ma, Y.; Wu, J.; Fan, L. *Compos. Appl. Sci. Manuf.* **2011**, *42*, 1398.
41. Wang, S. F.; Shen, L., Zhang, W. D.; Tong, Y. J. *Biomacromolecules* **2005**, *6*, 3067.
42. Wang, M. B.; Li, Y. B.; Wu, J. Q.; Xu, F. L.; Zuo, Y.; Jansen, J. A. *J. Biomed. Mater. Res. A* **2008**, *85A*, 418.
43. Satarkar, N. S.; Hilt, J. Z. *J. Control. Release* **2008**, *130*, 246.
44. Nel, A.; Xia, T.; Madler, L.; Li, N. *Science* **2006**, *311*, 622.
45. Mercer, R. R.; Scabilloni, J.; Wang, L.; Kisin, E.; Murray, A. R.; Schwegler-Berry, D.; Shvedova, A. A.; Castranova, V. *Am. J. Physiol. Lung Cell Mol. Physiol.* **2008**, *294*, L87.
46. Chen, X.; Schluesener, H. J. *Nanotechnology* **2010**, DOI 10.1088/0957-4484/21/10/105104.
47. Shvedova, A. A.; Castranova, V.; Kisin, E. R.; Schwegler-Berry, D.; Murray, A. R.; Gandelsman, V. Z.; Maynard, A.; Baron, P. *J. Toxicol. Environ. Health A* **2003**, *66*, 1909.
48. Kagan, V. E.; Tyurina, Y. Y.; Tyurin, V. A.; Konduru, N. V.; Potapovich, A. I. *Toxicol. Lett.* **2006**, *165*, 88.
49. Mejías Carpio, I. E.; Santos, C. M.; Wei, X.; Rodrigues, D. F. *Nanoscale* **2012**, *4*, 4746.
50. Meenach, S. A.; Anderson, A. A.; Suthar, M.; Anderson, K. W.; Hilt, J. Z. *J. Biomed. Mater. Res.* **2009**, *91A*, 903.
51. Pacurari, M.; Yin, X. J.; Zhao, J.; Ding, M.; Leonard, S. S.; Schwegler-Berry, D.; Ducatman, B. S.; Sbarra, D.; Hoover, M. D.; Castranova, V.; Vallyathan, V. *Environ. Health Perspect.* **2008**, *116*, 1211.